INSTITUT PASTEUR

Microbes and Infection 13 (2011) 85–95

www.elsevier.com/locate/micinf

Original article

Interaction between the yellow fever virus nonstructural protein NS3 and the host protein Alix contributes to the release of infectious particles

Lindsay N. Carpp [a,*], Ricardo Galler [b], Myrna C. Bonaldo [a]

[a] *Instituto Oswaldo Cruz/FIOCRUZ, Laboratório de Biologia Molecular de Flavivírus, Fundação Oswaldo Cruz, Avenida Brasil 4365, Manguinhos, RJ 21045-900, Brazil*

[b] *Vice-diretoria de Desenvolvimento Tecnológico, Bio-Manguinhos, Avenida Brasil 4365, Manguinhos, RJ 21045-900, Brazil*

Received 20 August 2010; accepted 2 October 2010
Available online 29 October 2010

Abstract

The ESCRT (endosomal sorting complex required for transport) machinery normally executes cargo sorting and internalization during multivesicular body biogenesis, but is also utilized by several enveloped viruses to facilitate their budding from cellular membranes. Although the mechanisms of flavivirus infectious particle assembly and release are poorly understood, the nonstructural protein NS3 has been reported to have an essential role via an undescribed mechanism. Here, we shed light on the role of NS3 by connecting it to the host factor Alix, a protein intimately connected with the ESCRT machinery. We demonstrate that NS3 and Alix interact and show that dominant negative versions of Alix inhibit YFV release. Furthermore, we show that NS3 supplied in *trans* rescues this effect. We propose that the interaction between NS3 and Alix contributes to YFV release.
© 2010 Institut Pasteur. Published by Elsevier Masson SAS. All rights reserved.

Keywords: Yellow fever virus; *Flavivirus*; Alix protein; Viral nonstructural proteins

1. Introduction

Yellow fever virus (YFV) is an enveloped RNA virus belonging to the Flaviviridae family and the *Flavivirus* genus. The YFV genome, a single-stranded positive sense RNA molecule of ~11 kb, is translated by the host cell into a single polyprotein which is cleaved by host and viral proteases, thereby generating the mature viral proteins [1]. The structural proteins (C, prM, and E) are incorporated into the virion, while the nonstructural proteins (NS1, NS2A, NS2B, NS3, NS4A, NS4B, and NS5) are important for RNA replication [1]. Flavivirus NS3 is a large (~70 kDa) multifunctional protein possessing helicase, protease, and RNA triphosphatase activities [2–4] and essential for viral replication [5]. In addition to these activities, a surprising role for NS3 in virus assembly/release was also demonstrated [6,7]; indeed, growing evidence suggests that nonstructural proteins are involved in particle morphogenesis (for review, see [8]). Although the mechanism of flaviviral particle morphogenesis is poorly understood, it is believed that the capsid protein associates with genomic RNA, acquires its host-derived envelope by budding into the lumen of the endoplasmic reticulum (ER), and exits via the secretory pathway [1]. Of particular note is the direction in which flavivirus particles are thought to be formed: by budding into the lumen of the ER and away from the cytosol, a physiologically unusual direction [1].

A topologically similar process occurs at the late endosomal membrane to sort membrane proteins bound for degradation into vesicles which invaginate into the endosomal lumen (and away from the cytosol), thereby generating a multivesicular body (MVB). This process is executed by the ESCRT proteins [9,10]. ESCRT proteins are recruited from the cytosol as complexes which act sequentially (ESCRT-0, -I, -II, and -III) and are required for MVB formation: ESCRT-0 and ESCRT-I recognize ubiquitinated proteins destined for degradation and also recruit downstream ESCRT machinery

* Corresponding author. Present address: Institute for Systems Biology, 1441 North 34th Street, Seattle, WA 98103, USA. Tel.: +1 206 732 1446; fax: +1 206 732 1299.
E-mail address: lcarpp@systemsbiology.org (L.N. Carpp).

1286-4579/$ - see front matter © 2010 Institut Pasteur. Published by Elsevier Masson SAS. All rights reserved.
doi:10.1016/j.micinf.2010.10.010

[11–13]. Likewise, the ESCRT-II complex interacts with components of ESCRT-III [14]. ESCRT-III subunits are recruited as soluble monomers and oligomerize on membranes [15], a process that has been proposed to promote the negative membrane curvature required for membrane budding [16]. These proteins are dissociated from the membrane by Vps4, an AAA-type ATPase [17]. Several other proteins are also intimately connected with the ESCRT machinery, including AIP1/Alix, a multifunctional protein that interacts with components of both ESCRT-I and ESCRT-III [18–20]. Altogether, the current model of ESCRT protein function proposes that they are involved in both initial cargo sorting events and the subsequent inward vesiculation/scission to generate the internal luminal vesicles of the MVB [10].

It is well documented that many viruses co-opt ESCRT machinery to facilitate their egress from cellular membranes. ESCRT proteins are recruited via conserved motifs which act as docking sites for cellular proteins to viral proteins; these motifs are termed late domains [21] because mutation of these motifs arrests viral budding at a late stage (i.e., scission of the virion from the host membrane). Three late domain consensus sequences within retroviral Gag proteins have been identified: PPxY, PT/SAP, and YPxL [21]. In addition to inhibiting viral budding, mutations in late domains also disrupt interaction with ESCRT proteins in a correlating manner [19,22]. Viruses also seem to have evolved multiple exit routes: Although human immunodeficiency virus type 1 (HIV-1) preferentially utilizes Tsg101 for budding [22], overproduction of Alix can rescue the release of HIV-1 when the Gag binding site for Tsg101 is mutated [23]. Therefore, it appears that multiple ESCRT and ESCRT-associated proteins can be used by the same virus.

Most work studying the role of ESCRT proteins in viral budding has focused on retroviruses which generally bud from the plasma membrane [21], and it is largely unknown whether the same machinery is used by viruses that bud from intracellular membranes, such as YFV. Recently, however, Alix was reported to be involved in the release of hepatitis B virus [24], a DNA virus which buds from intracellular membranes. It therefore seems likely that ESCRT-associated proteins may be broadly used by many viruses, not just retroviruses. In this study, we aimed to clarify the role of NS3 in YFV assembly by investigating its relationship with Alix. We show that NS3 associates with Alix using confocal microscopy and biochemical techniques. We also demonstrate that dominant negative versions of Alix inhibit the release of infectious YFV particles; furthermore, we show that NS3 supplied in *trans* can rescue this dominant negative effect. Our data therefore generate insight into the mechanism of YFV infectious particle production and lend further support to the idea that nonstructural proteins are involved in this process.

2. Materials and methods

2.1. Plasmids

The sequence encoding YFV NS3 (nt 4571-6439; Gen Bank accession no. X03700) was PCR amplified from pT3 [25] using oligos LC10 (5′ – **GCGGCCGCGC**CACC**ATG***GCC*A-GTGGGGATGTCTTGTG – 3′; ***Not*I** Kozak sequence (**start codon**), *alanine to remain in frame*) and LC8 (5′ – **GTCGAC**CCTCCTACCTTCAGCAAAC – 3′; ***Sal*I**). The *Sal*I site in the reverse primer was designed to insert the NS3 fragment in-frame with the C-terminal FLAG tag provided by the pFLAG-CMV-5a vector (Sigma). The 1.7 kb PCR product was subcloned first into pGEM-Easy (Promega) and then as a *Not*I/*Sal*I fragment into pFLAG-CMV-5a cut with the same enzymes. The S138A and R461Q mutations were introduced using the QuikChange mutagenesis kit (Stratagene) with oligos LC16/LC17 (5′ – CTTGACTATCCGAGTGGCACT**GCA**G-GATCTCCTATTGTTAAC – 3′/5′ – GTTAACAATAGGA-GATCC**TGC**AGTGCCACTCGGATAGTCAAG – 3′; **138A**) and LC14/LC15 (5′ – TCCGCATCCTCTGCTGCTCAA**CA-G**AGGGGGCGCATTGGGAGAAAT – 3′/5′ – ATTTCTC-CCAATGCGCCCCCT**CTG**TTGAGCAGCAGAGGATGCG-GA – 3′; **R461Q**), respectively. All mutations were verified by DNA sequencing.

For recombinant expression in *Escherichia coli*, the sequence encoding the helicase domain of NS3 (nt 5082-6439; Gen Bank accession no. X03700) was amplified from plasmid pT3 [25] using oligos RG113 (5′ – CG**GAATTC**ACTGAGGTGAAG-GAAGAAGG – 3′; ***Eco*RI**) and LC9 (5′ – **GTCGAC***TTAT-TA*CCTCCTACCTTCAGCAAAC – 3′; ***Sal*I**, *stop codons*). The ~1400 bp fragment was subcloned into pGEM-Easy (Promega) and further subcloned as an *Eco*RI/*Sal*I fragment into pET-28a (Novagen) cut with the same enzymes, generating pNS3-hel. The resulting construct produced the helicase domain of NS3 (residues 170–623) as an N-terminally His(6)-tagged fusion protein. The YPTI->APTA mutations were introduced as described above with oligos LC5 (5′–CAGGAAAACCTTTG AGAGAGAA**GCC**CCCACG**GCA**AAGCAGAAGAAACCTG AC – 3′; **399A, 402A**) and LC6 (reverse complement of LC5).

Constructs driving the expression of N-terminally EGFP-tagged Alix, N-terminally tagged HA-Alix and HA-Bro1V, and the N- and C-terminal domains of EGFP-Alix were generously provided by Prof. Wes Sundquist (University of Utah), Dr. Fadila Bouamr (National Institutes of Health) and Prof. Rémy Sadoul (Grenoble Institut des Neurosciences), respectively.

2.2. Antibodies

To raise polyclonal antibodies against NS3, a construct expressing N-terminally $His_{(6)}$-tagged NS3 was created. A fragment corresponding to nt 4571-6439 of the YFV cDNA was PCR amplified from pYFM5.2 [26] using oligos RG93 (5′ – CG**GAATTC**AGTGGGGATGTCTTGTG – 3′; ***Eco*RI**) and RG94 (5′– CCAATGCATTGG**CTGCAG**CCTCCTACCTT-CAGCA – 3′; ***Pst*I**) and subcloned into pDS56 [27]. NS3 was then produced recombinantly in *E. coli* and purified under denaturing conditions using Ni-NTA affinity chromatography. The resulting insoluble inclusion bodies (60 μg protein/ml) were resuspended in 2% SDS, 140 mM NaCl, and 2 mg/ml polyA–U and used to immunize rabbits. Anti-NS3 antibodies were concentrated through ammonium sulfate precipitation of

the serum from the second bleed. The resulting concentrate was dialyzed against PBS, divided into aliquots, and stored at −20 °C.

The following commercial antibodies were used: α-GFP, rabbit polyclonal (Invitrogen); α-HA, mouse monoclonal HA-7 (Sigma); α-FLAG, mouse monoclonal M2 (Sigma); and α-calnexin, rabbit polyclonal (Abcam).

2.3. Cell culture, transfection, and virus

Vero cells were maintained in Earle's 199 complete medium supplemented with 5% fetal bovine serum (FBS), in 5% CO_2. Transient transfections were performed with Lipofectamine 2000 (Invitrogen) according to the manufacturer's instructions. YF 17DD (Gen Bank accession ID: U17066) was used for infections.

2.4. Immunofluorescence and confocal microscopy

Vero cells were seeded (30,000 cells/cm^2) in 8-well Lab-Tek Chamber slides prior to transfection with plasmids driving the expression of NS3-FLAG and EGFP-Alix. Cells were fixed 24 h post-transfection with 3% para-formaldehyde in phosphate-buffered saline (PBS, 137 mM NaCl, 2.7 mM KCl, 4.3 mM Na_2HPO_4, 1.47 mM KH_2PO_4) pH 7.4. After washing, cells were permeabilized with 0.5% Triton X-100/PBS, washed, incubated in blocking solution [10% bovine serum albumin (BSA)/PBS], incubated in primary antibodies (monoclonal M2 α-FLAG, Sigma, diluted 1:1000 in 3% BSA/PBS), and washed. Secondary antibodies (α-mouse Alexa Fluor 546 conjugate, Invitrogen, 1:400 in 3% BSA/PBS) were added, followed by washing. Slow Fade DAPI reagent (Invitrogen) was used to mount the slides. Cells were visualized on a Zeiss LSM 510 confocal microscope and images were analyzed using Zeiss LSM Image Browser software.

For transfection/infection experiments, Vero cells were initially transfected as above with pEGFP-Alix. Five hours post-transfection, medium was removed and cells were infected with YF 17DD (moi = 0.1). Seventy-two hours post-infection, cells were fixed and immunolabeled as above. Anti-NS3 antibodies were used at 1:200. Secondary goat anti-rabbit Alexa Fluor 546 conjugated antibodies (Invitrogen) were used at 1:400.

2.5. Protein expression and purification

BL-21 cells were transformed with pNS3-hel, and protein expression was induced with 0.5 mM isopropyl β-D-1-thio-galactopyranoside when cultures reached mid-log phase (OD_{600} ~0.5–0.7). Cells were grown an additional 20 h at room temperature (~25° C). Cells were harvested, resuspended in buffer A (300 mM NaCl in PBS with 0.1% Tween 20, 25 μg/ml phenylmethanesulphonylfluoride (PMSF), 50 μM leupeptin, and 20 mM β-mercaptoethanol) and lysed by sonication. Cell lysates were spun at 4000*g* and further clarified through a 0.22 μ filter. His-tagged $NS3_{hel}$ was obtained by incubating clarified lysate with His-Select resin (Sigma) according to the manufacturer's instructions. Proteins were eluted with 250 mM imidazole in 300 mM NaCl/PBS and dialyzed against PBS. For protein concentration, sodium dodecyl sulfate polyacrylamide gel electrophoresis (SDS-PAGE) and Coomassie blue staining were used to compare purified proteins with a BSA standard curve. Quantity One software (Bio-Rad) was then used to determine protein concentrations.

2.6. Enzyme-linked immunosorbent assay (ELISA)

The purified helicase domain of NS3 (WT or APTA mutant) was diluted in coating buffer (0.1 M Na_2CO_3/0.1 M $NaHCO_3$, pH 9.6) and added (500 ng/well) to a 96-well polystyrene EIA/RIA plate (Corning Inc.). Plates were incubated overnight at 4 °C. Wells were washed with PBS (200 μl/well, including all subsequent washes) and blocked with 1% BSA/PBS. Wells were washed, and cell lysates from transiently transfected cells (EGFP-Alix), obtained at 24 h post-transfection, were serially diluted and added to wells. After incubation, wells were washed, and primary antibodies (rabbit polyclonal α-GFP, 1:1000 in 1% BSA/PBS) were added. Wells were washed, and secondary antibodies (goat α-rabbit HRP-conjugated, 1:1000 in 1% BSA/PBS) were added. Wells were washed, and 2,2′-azino-bis [3-ethylbenziazoline-6-sulfonic (ABTS) acid peroxidase solution (Kirkegaard and Perry Laboratories) was added (50 μl/well). Reactions were incubated at RT and stopped with 1% SDS. Absorbances (at 405 nm) were obtained through spectrophotometric measurement. After subtracting background values (obtained by lysate of mock-transfected cells binding to each version of $His_{(6)}$-$NS3_{hel}$), the highest absorbance in each experiment was set to 100%, and all other values were expressed as percentages. Negative values were set to zero. Nonlinear regression curve fits (one site, specific binding) were obtained with GraphPad Prism.

2.7. Coimmunoprecipitations

Vero cells were seeded in 6-well plates and subsequently transfected with pEGFP-C2 (Clontech) or pEGFP-Alix. Five hours post-transfection, medium was removed and cells were infected with YFV 17DD (moi = 0.1). At 72 h post-infection, cells were lysed in 50 mM Tris–HCl pH 7.5, 150 mM NaCl, 1 mM ethylenediamine tetraacetic acid (EDTA), 0.25% Triton X-100, 25 μg/ml PMSF, 50 μM leupeptin. Lysates were vortexed and clarified in a benchtop microfuge. Protein A-agarose resin (Invitrogen) was blocked by incubating in 1% BSA/PBS for 15 min. Following lysate preclearing, 200 μl of each lysate were combined with an additional 200 μl of lysis buffer and either 10 μl of polyclonal α-NS3 antibodies, or 1 μl of polyclonal α-GFP antibodies. Lysates and antibodies were rotated for 2 h at 4 °C, then 50 μl of pre-blocked Protein A-agarose were added and rotated. After washes, bound proteins were eluted with Laemmli sample buffer with 5% β-mercaptoethanol. Proteins were denatured for 5 min at 95 °C and resolved by SDS-PAGE, followed by transfer to nitrocellulose membrane and Western blot analysis.

2.8. Western blotting

To obtain cellular extracts, cells were washed and lysed (~5 × 10^6 cells/ml). Lysates were vortexed for 1 min and clarified by spinning for 1 min at top speed in a benchtop microfuge, then mixed with 4× Laemmli buffer and heated for 5 min at 95 °C. Proteins in cellular extracts were then resolved by SDS-PAGE and subsequently transferred to nitrocellulose membranes. Nonspecific sites on membranes were blocked with 5% nonfat milk in PBST (PBS pH 7.4, 0.5% Tween 20). Primary antibodies were diluted in 1% nonfat milk/PBST prior to incubation with membranes. Followed by extensive washing with PBST, membranes were incubated with secondary (goat α-rabbit HRP-conjugated, Amersham Biosciences; goat α-mouse HRP-conjugated, Sigma) antibodies diluted in 5% nonfat milk/PBST. Membranes were washed extensively with PBST and then visualized with enhanced chemiluminescence (Amersham Biosciences) and autoradiography.

2.9. Transfection/infection experiments

Vero cells were seeded (50,000 cells/cm^2) in 6-well plates one day prior to transfection with pcDNA3 (Invitrogen), HA-Alix, HA-Bro1V, pEGFP-C2, pEGFP-ALIX NT, or pEGFP-ALIX CT. Five hours post-transfection, medium was removed and cells were infected with YFV 17DD (moi = 0.02) by incubating cells with virus for 1 h at 37 °C with rocking every 15 min. At the end of the incubation, medium was removed and cells were washed to remove unbound virus. To determine extracellular virus titers, samples of culture supernatants were taken at 72 h post-infection, clarified for 5 min at 2800*g*, and stored at −80 °C until titers were determined by plaque assays on Vero cells.

2.10. Plaque assays

Culture supernatants were serially diluted in medium and added to Vero cell monolayers. Virus was allowed to adsorb for 1 h at 37 °C/5% CO_2, with rocking. Excess virus was then removed and a carboxymethylcellulose (CMC) overlay (Earle's 199/5% fetal bovine serum/3% CMC) was applied. Plates were incubated for 6 days before fixing in 5% formaldehyde and staining with 0.04% crystal violet (Sigma–Aldrich) prior to plaque counting.

2.11. qRT-PCR

Intracellular RNA was extracted from ~5 × 10^5 cells at 48 h post-infection using an RNAqueous® Kit (Applied Biosystems). To detect viral genomic RNA, reverse-transcription followed by real-time PCR with YFV-specific primers was performed. Reactions were performed in a 20 μl volume and contained 2 μl of RNA preparations (1:50) and TaqMan® One-Step RT-PCR Master Mix Reagents (Applied Biosystems). Primers fwdYF-17D10188 (5′ – GCGGATCACTGATTGGAATGAC – 3′) and revYF-17D10264 (5′ – CGTTCGGATACGATGGATGACTA – 3′) were designed to amplify a 77 bp fragment of NS5 (nt 10188–10264 in the YF 17DD genome) and were used at 0.3 μM (final) each. A FAM/TAMRA TaqMan® probe was used at 0.25 μM (5′ – 6FAM-AATAGGGCCACCTGGGCCTCCC-TAMRA – 3′). Cellular 18S ribosomal RNA (18S rRNA) was also amplified using ribosomal RNA control reagents (Applied Biosystems). Reactions were carried out in an ABI Prism 7000 cycler (Applied Biosystems). Yellow fever virus data were normalized to an internal control using Pfaffl's method [28]. Ratios were $\log_{(2)}$ transformed and averaged to yield mean ratios.

3. Results

3.1. Colocalization of NS3 and Alix

We reasoned that the function of NS3 reported to be required for the release of infectious particles [7] may be the recruitment of host cell factors involved in the liberation of other enveloped viruses, e.g. ESCRT proteins. We decided to begin by investigating whether YFV NS3 colocalized with Alix, a protein physically connected with both ESCRT-I and ESCRT-III [18–20]. As an initial approach to answer this question, cells were cotransfected with constructs driving the expression of NS3-FLAG and EGFP-Alix. Using confocal microscopy, we observed that these proteins colocalized (Fig. 1A). Seeking more authentic conditions under YFV infection, we then performed a similar experiment in YFV-infected cells. We first verified that our α-NS3 antibodies did not stain mock-infected cells nonspecifically (Fig. 1B). We then transfected cells with EGFP-Alix and subsequently infected them with YFV. We observed that NS3 was present in the perinuclear region and that NS3 and EGFP-Alix often colocalized in the perinuclear region or punctate structures (Fig. 1C–E). This suggested that NS3 and Alix are associated in YFV-infected cells.

3.2. Biochemical association of NS3 and Alix

We next investigated whether Alix and NS3 associated in lysates from YFV-infected cells. Vero cells were transiently transfected with EGFP-Alix (or pEGFP-C2 as a negative control) and subsequently infected with YFV. At 72 h post-infection, cell lysates were prepared and proteins were immunoprecipitated with either α-NS3 or α-GFP antibodies. Bound proteins were subsequently analyzed by SDS-PAGE and Western blotting with α-NS3 antibodies. Our α-NS3 antibodies recognized a protein migrating at the correct apparent molecular weight (71 kDa) found exclusively in lysates from YFV-infected cells compared to mock-infected cells (Fig. 2A, lane 2 compared to lane 1). An additional band of approximately 50 kDa was also recognized in mock and infected cell lysates (Fig. 2A, lanes 1 and 2), representing a nonspecific cross-reacting protein. Our α-NS3 antibodies also efficiently immunoprecipitated NS3 from a lysate from cells infected with YFV and expressing EGFP-Alix (lane 3); importantly, NS3 could also be coimmunoprecipitated from the same lysate using α-GFP antibodies (lane 4). No band migrating at the same apparent molecular weight of NS3 was

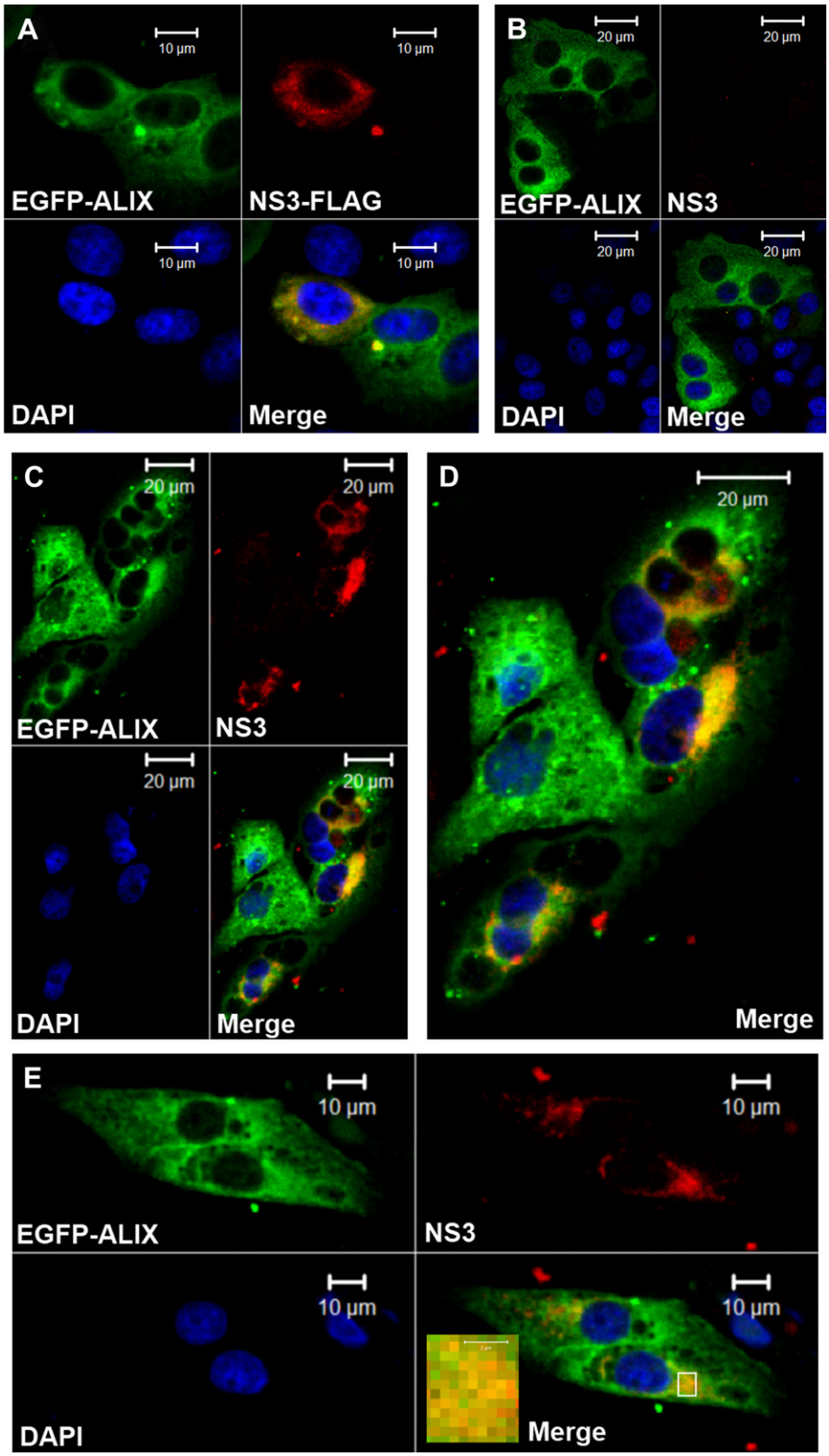

Fig. 1. Colocalization of NS3 and Alix. A) Immunofluorescence showing that NS3-FLAG (red) and EGFP-Alix (green) colocalize (yellow) in Vero cells transiently expressing the two proteins. Nuclei (blue) were counterstained with DAPI for reference. Scale bars, 10 µm. B) α-NS3 antibodies do not stain mock-infected cells. Vero cells transfected with EGFP-Alix were mock infected and stained with α-NS3 antibodies. Nuclei (blue) were counterstained with DAPI for reference. Scale bars, 20 µm. C—E) Colocalization of NS3 and EGFP-Alix in YFV-infected cells. Vero cells transfected with EGFP-Alix were infected with YF 17DD (moi = 0.1). Cells were fixed and stained with α-NS3 antibodies. Nuclei (blue) were counterstained with DAPI for reference. Scale bars, 20 µm. D) An enlarged version of the merge of (C). Scale bar, 20 µm. E) As in (C). Scale bars, 10 µm. The inset of the lower right panel shows an enlarged version of the region outlined in white in the merge of (E). Scale bar, 2 µm. (For interpretation of the references to colour in this figure legend, the reader is referred to the web version of this article.)

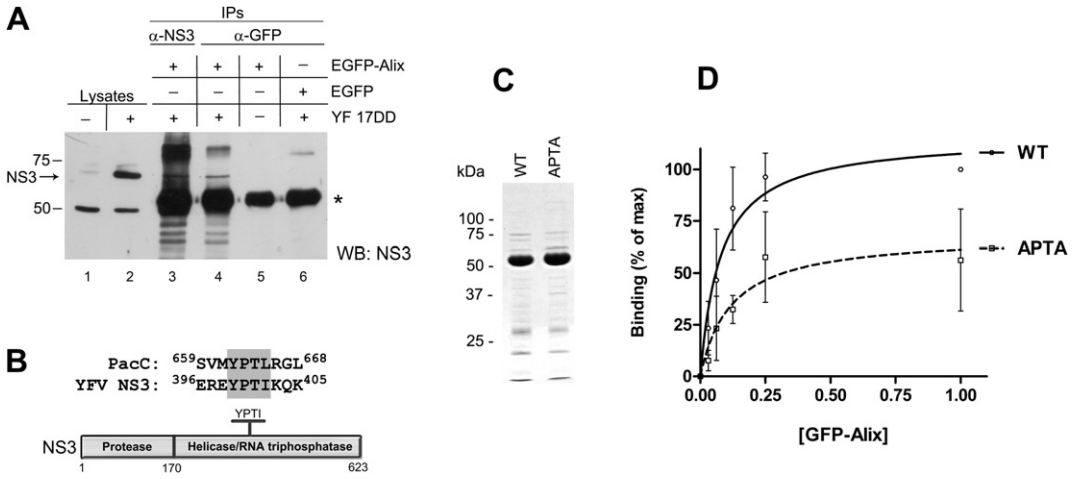

Fig. 2. Interaction between NS3 and Alix. A) Coimmunoprecipitation of EGFP-Alix and NS3 in lysates from YFV-infected cells. The membrane has been probed with α-NS3 antibodies. Lanes 1 and 2: Cell lysates of mock- (1) and YF 17DD-infected (2) Vero cells. Lane 3: NS3 immunoprecipitated with α-NS3 antibodies from a lysate of cells infected with YF 17DD and expressing EGFP-Alix. Lane 4: NS3 coimmunoprecipitated with α-GFP antibodies from the same lysate as in (3). Note: 1.25% of the lysate input for lanes (3) and (4) is loaded in lane (2). Lanes 5 and 6: No NS3 is coimmunoprecipitated with α-GFP antibodies from a lysate of (5) mock-infected cells expressing EGFP-Alix, or (6) YF 17DD-infected cells expressing EGFP alone. The asterisk shows the position of the heavy chain of the α-NS3/α-GFP antibodies used in the immunoprecipitations. B) Sequence alignment showing conservation of residues ("YPxL/I") found to be critical for PacC interaction with Alix [29] in NS3. Below: schematic diagram of the domains of NS3. The N-terminal third of the protein constitutes the serine protease domain, while the C-terminal two-thirds have helicase and RNA triphosphatase activities [1]. The approximate location of the YPTI motif in the helicase domain is shown. C,D) The YPTI motif in NS3 is involved in its interaction with Alix. The helicase domain of NS3 (WT, or harboring the $_{399}$YPTI$_{402}$ → $_{399}$APTA$_{402}$ mutation) was produced recombinantly in *E. coli* (C) and adsorbed to an ELISA plate. The binding of EGFP-Alix, provided by a cell lysate of transiently transfected cells, was then examined to each version of NS3$_{hel}$ (D). Data shown are compiled from three independent experiments, each performed at least in duplicate. Error bars represent ±SEM.

immunoprecipitated with α-NS3 antibodies from a lysate of mock-infected cells expressing EGFP-Alix (lane 5). Furthermore, the coimmunoprecipitation of NS3 with EGFP-Alix was not due to nonspecific interaction with the EGFP tag, since α-GFP antibodies did not coimmunoprecipitate NS3 in a lysate from cells infected with YFV and expressing EGFP alone (lane 6). These data suggest that NS3 and Alix interact, either directly, or as part of a complex.

We next inspected the amino acid sequence of YFV NS3 for possible motifs which might mediate a direct interaction with Alix. The equine infectious anemia virus (EIAV) p9 protein has been demonstrated to interact with Alix via YPxL sequence [18–20], and we found a YPTI sequence in YFV NS3 starting at residue 399 (Fig. 2B). This sequence also matches the YPxL/I core motif (Fig. 2B) in the transcription factor PacC which mediates its interaction with Alix [29]. To investigate the function of the YFV NS3 YPTI motif, we performed ELISAs to compare the binding of NS3$_{WT}$ and NS3$_{YPTI}$ → $_{APTA}$ to Alix. The helicase domain of NS3 (residues 170–623, His$_{(6)}$-NS3$_{hel}$) was produced recombinantly in *E. coli* as a His$_{(6)}$ fusion protein (Fig. 2C), purified, and immobilized on a 96-well ELISA plate. We then investigated the binding of EGFP-Alix, provided by a lysate of transiently transfected cells, to His$_{(6)}$-NS3$_{hel}$. We found a dose-dependent association of EGFP-Alix with His$_{(6)}$-NS3$_{hel}$ WT (Fig. 2D), suggesting that the two proteins interact directly. When two residues of the NS3$_{YPTI}$ motif were mutated to alanines (APTA), the affinity of this interaction decreased (Fig. 2D), suggesting that the YPTI motif in YFV NS3 contributes to its interaction with Alix.

3.3. Effect of dominant negative versions of Alix on infectious YFV particle release

We next sought a technique to investigate the functional relevance of the interaction between NS3 and Alix. Attempts to mutate the YPTI motif in NS3 in the YFV genome did not yield viable virus (data not shown), so truncated versions of Alix were introduced into cells prior to infection with YFV and their effects on the production of infectious particles were determined. Alix is composed of three domains (Fig. 3A); an N-terminal Bro1 domain, a central V domain, and a C-terminal proline-rich domain (PRD). The central V domain interacts with retroviral Gag proteins HIV-1 p6 and EIAV p9 [23,30], while Alix is linked to the ESCRT machinery via its Bro1 and PRD domains: Alix interacts directly with Tsg101, a component of ESCRT-I, via its PRD [18–20]; whereas Alix interacts with CHMP4, a component of ESCRT-III, via its Bro1 domain [31,32]. Therefore, truncated versions of Alix lacking binding sites for one of these components could have a dominant negative effect. We transiently transfected Vero cells with constructs driving the expression of full-length (HA-Alix), N-terminal (EGFP-NT), Bro1V (HA-Bro1V), and C-terminal (EGFP-CT) versions of Alix (Fig. 3A). Transfected cells were subsequently infected with YFV and viral titers in the cell culture supernatant were determined at 72 h post-infection by plaque assays on Vero cells. None of the truncated versions of Alix affected viral protein expression (NS3, Fig. 3B); however, we found that production of either the Bro1V or the C-terminal domain of Alix decreased the titer of infectious YFV by approximately 35% compared to the empty

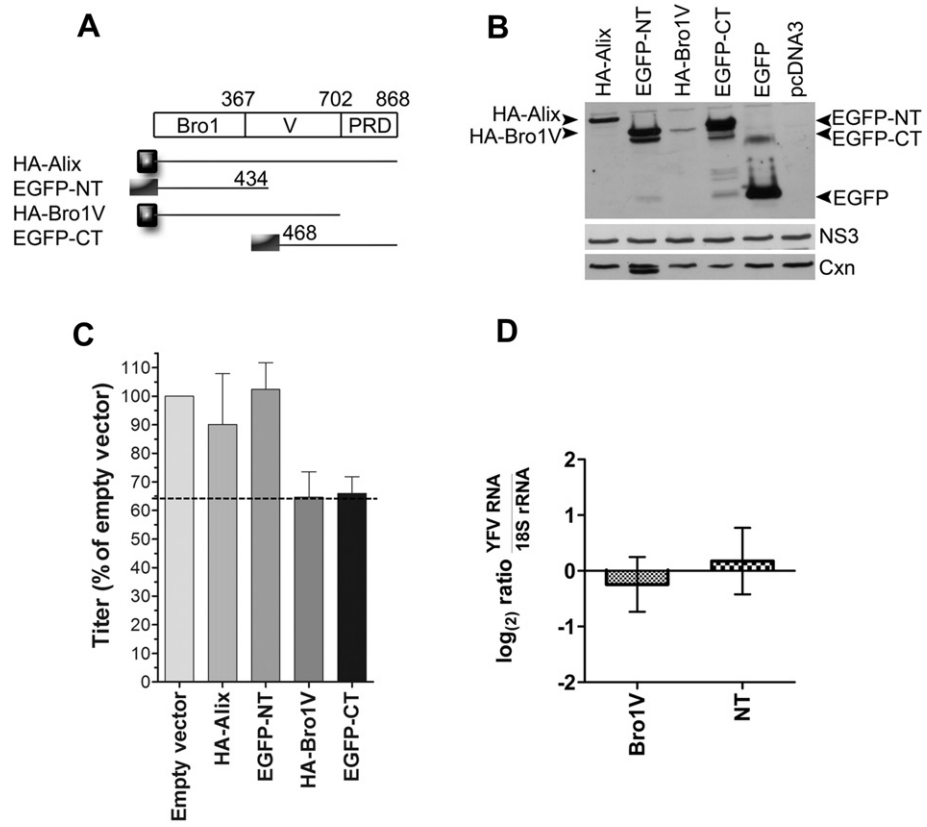

Fig. 3. Truncated versions of Alix inhibit the release of YFV without affecting replication. A) Schematic diagram of the domains of Alix and the truncations used in this study. Bro1, Bro1 domain; V, V domain; PRD, proline-rich domain. B) Western blot analysis of cell lysates from cells used in (C) showing expression of truncated versions of Alix. Membranes were probed with a mixture of α-HA and α-GFP antibodies (upper panel). Membranes were stripped and probed with α-calnexin antibodies as a loading control (bottom panel). Membranes were then stripped once more and probed with α-NS3 antibodies (middle panel). C) Production of HA-Bro1V and EGFP-CT decreases the titer of extracellular YFV infectious particles. Vero cells were transiently transfected with constructs expressing various truncations of Alix and subsequently infected with YF 17DD. Samples of cell culture supernatants were taken at 72 h post-infection and YFV titers were determined by plaque assays on Vero cell monolayers. Titers are expressed as % of titer obtained from cells transfected with empty vector (pcDNA3 or pEGFP-C2, as appropriate). Data shown are one representative experiment from at least three independent experiments for each truncation. Error bars represent ±SD. D) Detection of intracellular YFV RNA via qRT-PCR. Cells were transfected and infected as in (B) and intracellular RNA was extracted at 48 h post-infection. YFV RNA was then detected via qRT-PCR using NS5-specific primers. YFV data were normalized to 18S rRNA data using Pfaffl's method, and ratios were $\log_{(2)}$ transformed and averaged to yield the mean ratios shown in 4D. Data shown are the averages of at least three independent experiments for each truncation. Error bars represent ±SEM.

vector controls (Fig. 3C). In contrast, production of the N-terminal domain of Alix or overproduction of the full-length protein did not affect the titer of YFV released (Fig. 3C).

To determine whether HA-Bro1V interfered with infectious particle release as opposed to prior steps in the virus life cycle, such as replication, intracellular viral RNA was quantitated using real-time reverse-transcription PCR (qRT-PCR). Cells were transfected and infected as above, and intracellular RNA was extracted from cells at 48 h post-infection. YFV RNA was then quantitated by qRT-PCR using YFV-specific primers. The N-terminal domain of Alix was used as a control whose presence did not affect the release of infectious YFV (Fig. 3C). No significant difference in the quantity of YFV viral RNA was seen in cells transfected with Bro1V or empty vector (Fig. 3D), suggesting that the presence of Bro1V does not inhibit viral replication. Altogether, our data suggest that dominant negative versions of Alix do not inhibit viral replication or protein expression; rather, they decrease the amount of infectious particles liberated.

3.4. NS3 supplied in trans *rescues the dominant negative effect of Bro1V*

We next sought to gain insight into the mechanism of the dominant negative effect of HA-Bro1V on YFV infectious particle release. We hypothesized that if the introduction of HA-Bro1V into cells saturated NS3 binding sites non-productively, NS3 supplied in *trans* could restore the release of virus. To this end, Vero cells were cotransfected with constructs driving the expression of HA-Bro1V and NS3-FLAG (and/or empty vectors as appropriate), infected with YFV, and the titers of the infectious YFV particles released into the culture supernatant were determined by plaque assay.

We found that *trans*-supplied NS3-FLAG did indeed relieve the dominant negative effect introduced by HA-Bro1V (Fig. 4A), suggesting that NS3 acts in concert with Alix to effect YFV infectious particle release. To examine whether the known enzymatic activities of NS3 were required for this rescue function, two mutant versions of NS3 were constructed.

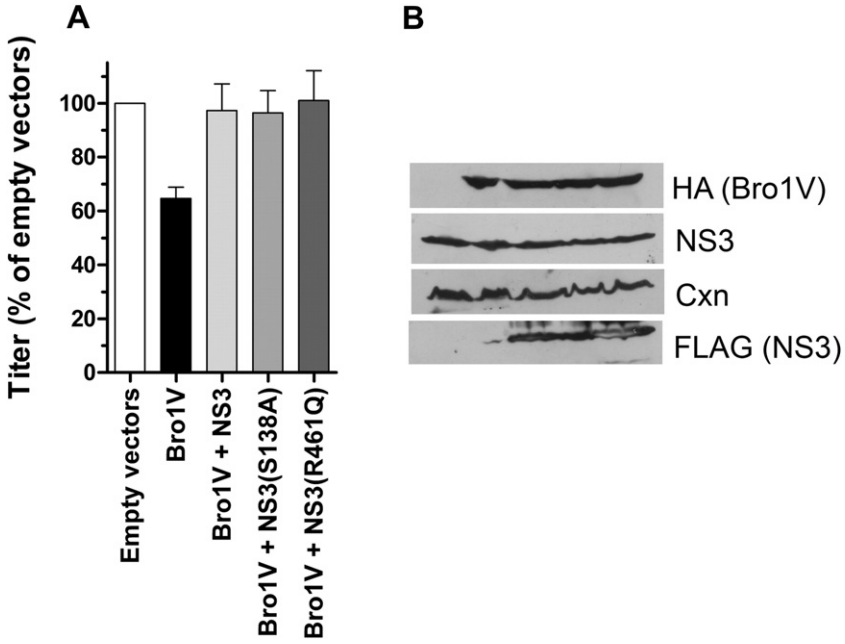

Fig. 4. Production of NS3 in *trans* relieves the dominant negative effect of Bro1V. A) Vero cells were transiently cotransfected with constructs expressing HA-Bro1V, NS3-FLAG (and various mutant versions thereof), or empty vector as appropriate and subsequently infected with YF 17DD. Samples of cell culture supernatants were taken at 72 h post-infection and YFV titers were determined by plaque assay on Vero cells. Titers are expressed as % of titer obtained from cells cotransfected with empty vectors. Data shown are the combined results of three independent experiments. Error bars represent ±SEM. B) Western blot analysis of cell lysates (top three panels) and Triton X-insoluble fractions (bottom panel) from the cells used in (A). Proteins in cell lysates were resolved by SDS-PAGE and transferred to nitrocellulose membrane. The membrane was probed with α-HA antibodies (top panel), stripped and probed with α-NS3 antibodies (second panel), and stripped once more and probed with α-calnexin (cxn) antibodies (third panel). Bottom panel: Proteins in the Triton X-insoluble fraction from the cells used in (A) were solubilized in Laemmli buffer through sonication in a water bath, denatured, and resolved by SDS-PAGE. After transfer to nitrocellulose membrane, the blot was probed with α-FLAG antibodies (bottom panel).

One of these, NS3 S138A, contains a point mutation in the catalytic triad that renders the serine protease activity of NS3 inactive [2]. The second, NS3 R461Q, contains a point mutation in a region that is thought to be involved in ATP binding [33]. Both versions of NS3 were also capable of relieving the dominant negative effect caused by HA-Bro1V (Fig. 4A), providing further support to the idea that NS3 fulfills a function in virus release in cooperation with host cell machinery.

4. Discussion

Our data indicate that Alix, a protein used by several retroviruses to facilitate their budding, can bind to the YPTI motif in NS3 (Fig. 2). We took advantage of the reported crystal structure of YFV NS3 [33] to spatially locate this motif and relate it to other functional motifs present in this protein (Fig. 5). The YFV NS3 helicase, like other flaviviral helicases, is composed of three different domains (Fig. 5A–C): domain 1 (residues 187–327), domain 2 (residues 328–488) and domain 3 (residues 489–623). The YPTI Alix-binding motif is localized between the third and the fourth β strands of the domain 2, in the β3 β4 loop, encompassing residues 390–408 (Fig. 5A–C). Part of this solvent-accessible loop, residues 397–404 (REYPTIKQ, containing the YPTI motif), exhibits a disordered structure and was not included in the structural model of the YFV NS3 helicase [33]. However, residues 390–396 and 405–408 are included (Fig. 5A).

This YPTI bearing loop has a distinct location in relation to the seven conserved helicase sequence motifs present around the interdomain cleft formed by domains 1 and 2. The catalytic core is involved in NTP binding and hydrolysis and coupling the NTPase to RNA duplex unwinding [4]. The YPTI-β3 β4 loop is localized in front of this helicase catalytic center, protruding out of the helicase, above the groove that binds double-stranded RNA [34]. Another functional motif located near the YPTI loop in domain 2 is the β1 α1 loop (residues 342–353), which has already been implicated in viral assembly/release in two previous works [6,7]. A second-site change of NS3 residue D343 suppressed a defect in particle release caused by a mutation in NS2A [6], whereas mutation of NS3 W349 selectively blocked the release of infectious particles [7]. These two loops are spatially separated by α2, which is a larger alpha-helix placing laterally away from domain 2.

It will also be interesting to determine whether other ESCRT components interact with YFV proteins. It is worth noting that Tsg101, a subunit of ESCRT-I, has been demonstrated to interact with NS3 of a closely related flavivirus, Japanese encephalitis virus [35]. However, sequence analysis of YFV NS3 did not reveal any of the PT/SAP motifs known to be responsible for binding to Tsg101 (data not shown). The alignment of domain 2 from selected flaviviral NS3 helicases

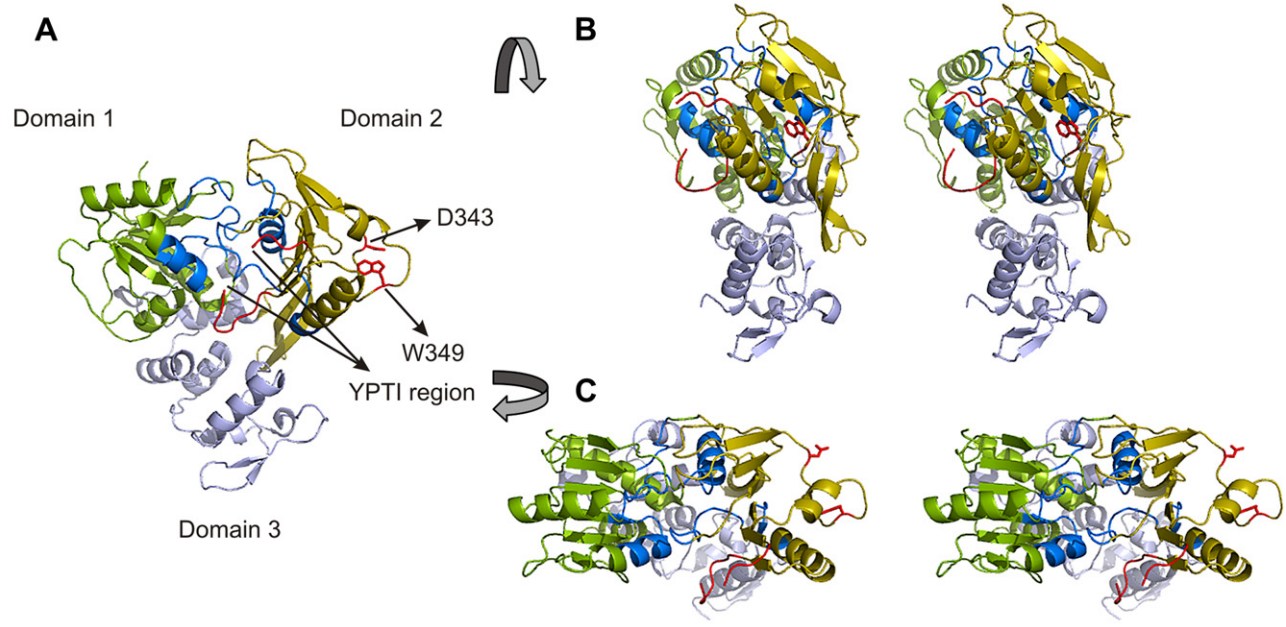

D

```
                                                                IV
                          β1                  α1        β2          α2              β3
                        EEEEE               HHHHH     EEEE    HHHHHHHHHHHHH     EEE
YF    328DEFPHSNGEIEDVQTDIPSEPWNTGHDWILADKRPTAWFLPSIRAANVMAASLRKAGKSVVVLNRKTFERE YPTI KQKKPD
DEN2  323DPFPQSNAPIMDEEREIPERSWNSGHEWVTDFKGKTVWFVPSIKAGNDIAACLRKNGKKVIQLSRKTFDSEYIKTRTNDWD
DEN4  323DPFPQSNSPIEDIEREIPERSWNTGFDWITDYQGKTVWFVPSIKAGNDIANCLRKSGKRVIQLSRKTFDTEYPKTKLTDWD
JE    324DPFPDSNAPIHDLQDEIPDRAWSSGYEWITEYAGKTVWFVASVKMGNEIAMCLQRAGKKVIQLNRKSYDTEYPKCKNGDWD
MVV   324DPFPDTNSPVHDVSSEIPDRAWSSGFEWITDYAGKTVWFVASVKMSNEIAQCLQRAGKRVIQLNRKSYDTEYPKCKNGDWD
KUN   324DPFPESNAPISDLQTEIPDRAWNSGYEWITEYIGKTVWFVPSVKMGNEIALCLQRAGKKVIQLNRKSYETEYPKCKNDDWD
      324* **.:*. : * . :**...*.:*.:*:      *.**:.*:: .* :* .*:: ** *: *.**::: ** . :  . *

                V                                                  VI
      β4                  β5      β6              β7          α3                  β8
     EEEE                EEEE   EEEEEEEE      EEEEEEEEE   HHHHHHHH           EEEEE
YF    FILATDIAEMGANLCVERVLDCRTAFKPVLVDEGR-KVAIKGPLRISASSAAQRRGRIGRNPNRDGDSYYYSEPTSENNAH488
DEN2  FVVTTDISEMGANFKAERVIDPRRCMKPVILTDGEERVILAGPMPVTHSSAAQRRGRVGRNPKNENDQYIYMGEPLENDED484
DEN4  FVVTTDISEMGANFRAGRVIDPRRCLKPVILTDGPERVILAGPIPVTPASAAQRRGRIGRNPAQEDDQYVFSGDPLKNDED484
JE    FVITTDISEMGANFGASRVIDCRKSVKPTILEEGEGRVILGNPSPITSASAAQRRGRVGRNPNQVGDEYHYGGATSEDDSN485
MVV   FVITTDISEMGANFGASRVIDCRKSVKPTILDEGEGRVILSVPSAITSASAAQRRGRVGRNPSQIGDEYHYGGGTSEDDTM485
KUN   FVVTTDISEMGANFKASRVIDSRKSVKPTIITEGEGRVILGEPSAVTAASAAQRRGRTGRNPSQAGDEYCYGGHTNEDDSN485
      *:::***:*****: . **:* * ..**.:: :*  :* :  *  :: :******** **** . .*.* :   . :::
```

Fig. 5. Structure and functional motifs of YFV NS3 helicase. A) The ribbon diagram of the YFV NS3 helicase based on the PDB entry 1YKS [33]. Domain 1 is shown in yellow, domain 2 is green, and domain 3 is light blue. The seven helicase motifs are colored in cyan. The YPTI bearing β3 β4 solvent-accessible loop of domain 2 (residues 390–408) is highlighted in red. The assembly-related residues D343 and W349 of the β1 α1 loop (residues 342–353) are also shown in red. B) Stereo ribbon diagram of lateral and (C) top views of YFV NS3 helicase. Pymol software (DeLano Scientific) was used to generate these figures. D) Structure-based alignment of flaviviral NS3 helicases determined by the TCoffee program [44]. The amino acid sequences of dengue 2 virus (DEN2; entry 2BMF), dengue 4 virus (DEN4; entry 2JLQ), Japanese encephalitis virus (JE; entry 2Z83), Murray Valley encephalitis virus (MVV; entry 2V8O), Kunjin virus (KUN, entry 2QEQ) and yellow fever virus (YF; entry 1YKS) were obtained from PDB. YFV NS3 helicase secondary structure elements are indicated above the alignment. The conserved helicase motifs IV,V and VI localized in domain 2 are highlighted in blue. The YF NS3 helicase residues D434 and W349 as well as the YPTI motif are shown in red. Under the alignment, the following symbols denote the degree of conservation observed at each amino acid position: (*) identical in all sequences; (:) conserved substitutions and (.) semi-conserved substitutions. (For interpretation of the references to colour in this figure legend, the reader is referred to the web version of this article.)

indicates that the motif YPTI is only present in the YFV protein (Fig. 5D). Dengue 2 and dengue 4 virus NS3 helicases present the motifs YIKT and YPKT, respectively. The sequence YPKC is present in all the selected Japanese encephalitis virus group helicases. It would also be interesting to determine whether these motifs are also capable of interacting with Alix.

Introduction of dominant negative versions of Alix into cells prior to infection with YFV decreased the extracellular titer of YFV compared to controls (~35%, Fig. 3). This finding

is consistent with a study of HBV, in which a similar Bro1V version of Alix inhibited the extracellular release of HBV virions by approximately 40% [24]. In other viruses such as HIV-1, introduction of Bro1V has a stronger (approximately 70%) inhibitory effect on virus particle release [36]. In our experiments, dominant negative effects may be masked by the population of cells which are infected but not transfected (between 30 and 40% as assessed by flow cytometry, data not shown), or by the presence of the endogenous Alix *Cercopithecus aethiops* ortholog. Further studies to investigate the effect of Alix gene silencing on YFV release are planned to address this.

Importantly, we also showed that NS3 supplied in *trans* could rescue the defect in infectious particle release conferred by Bro1V (Fig. 4). To the best of our knowledge, this is the first example of a nonstructural protein rescuing a release defect conferred by a dominant negative version of an ESCRT related protein, although at least one other example of a nonstructural protein interacting with an ESCRT protein to facilitate virus release has been reported [37]. We propose that NS3 recruits Alix to aid in the release of infectious particles, like many other viruses shown to use ESCRT and ESCRT-associated proteins for their budding [21]. NS3 is likely present at sites of particle assembly, as cleavage of the C-prM junction by NS2B-NS3 is absolutely required for infectious particle release [38,39]. Once recruited to the site of particle assembly, Alix could perform various roles to aid in particle release: 1) recruiting ESCRT-III and Vps4, thereby driving virion scission [40], or 2) recruiting endophilins [41], which generate membrane curvature [42,43], thereby aiding initial steps in budding. Further studies will be needed to test these hypotheses.

Acknowledgements

We are grateful to Prof. Wes Sundquist, Dr. Fadila Bouamr, and Prof. Rémy Sadoul for generously providing plasmids. We thank Igor dos Santos Cestari for critical reading of the manuscript and Juliana Ribeira dos Santos for technical assistance. We acknowledge Regiane Burger for obtaining the α-NS3 antibodies and the Plataforma de Seqüenciamento de DNA PDTIS/FIOCRUZ for DNA sequencing. This work was supported by FIOCRUZ, the Instituto de Ciência e Tecnologia de Vacina (INCTV - CNPq/MCT), and a postdoctoral fellowship (E-26/100.015/2009) from FAPERJ to LNC.

References

[1] B.D. Lindenbach, H. Thiel, C.M. Rice, Flaviviridae: the viruses and their replication (33). in: D.M. Knipe, P.M. Howley (Eds.), Fields Virology. Lippencott-Raven Publishers, Philadelphia, 2007, pp. 1101–1152.

[2] T.J. Chambers, R.C. Weir, A. Grakoui, D.W. McCourt, J.F. Bazan, R.J. Fletterick, C.M. Rice, Evidence that the N-terminal domain of nonstructural protein NS3 from yellow fever virus is a serine protease responsible for site-specific cleavages in the viral polyprotein, Proc. Natl. Acad. Sci. U S A 87 (1990) 8898–8902.

[3] T.J. Chambers, A. Grakoui, C.M. Rice, Processing of the yellow fever virus nonstructural polyprotein: a catalytically active NS3 proteinase domain and NS2B are required for cleavages at dibasic sites, J. Virol. 65 (1991) 6042–6050.

[4] D. Luo, T. Xu, R.P. Watson, D. Scherer-Becker, A. Sampath, W. Jahnke, S.S. Yeong, C.H. Wang, S.P. Lim, A. Strongin, S.G. Vasudevan, J. Lescar, Insights into RNA unwinding and ATP hydrolysis by the flavivirus NS3 protein, EMBO J. 27 (2008) 3209–3219.

[5] A.E. Matusan, M.J. Pryor, A.D. Davidson, P.J. Wright, Mutagenesis of the dengue virus type 2 NS3 protein within and outside helicase motifs: effects on enzyme activity and virus replication, J. Virol. 75 (2001) 9633–9643.

[6] B.M. Kummerer, C.M. Rice, Mutations in the yellow fever virus nonstructural protein NS2A selectively block production of infectious particles, J. Virol. 76 (2002) 4773–4784.

[7] C.G. Patkar, R.J. Kuhn, Yellow Fever virus NS3 plays an essential role in virus assembly independent of its known enzymatic functions, J. Virol. 82 (2008) 3342–3352.

[8] C.L. Murray, C.T. Jones, C.M. Rice, Architects of assembly: roles of Flaviviridae non-structural proteins in virion morphogenesis, Nat. Rev. Microbiol. 6 (2008) 699–708.

[9] J.H. Hurley, S.D. Emr, The ESCRT complexes: structure and mechanism of a membrane-trafficking network, Annu. Rev. Biophys. Biomol. Struct. 35 (2006) 277–298.

[10] P.I. Hanson, S. Shim, S.A. Merrill, Cell biology of the ESCRT machinery, Curr. Opin. Cell Biol. 21 (2009) 568–574.

[11] D.J. Katzmann, C.J. Stefan, M. Babst, S.D. Emr, Vps27 recruits ESCRT machinery to endosomes during MVB sorting, J. Cell Biol. 162 (2003) 413–423.

[12] D.J. Katzmann, M. Babst, S.D. Emr, Ubiquitin-dependent sorting into the multivesicular body pathway requires the function of a conserved endosomal protein sorting complex, ESCRT-I, Cell 106 (2001) 145–155.

[13] H. Teo, D.J. Gill, J. Sun, O. Perisic, D.B. Veprintsev, Y. Vallis, S.D. Emr, R.L. Williams, ESCRT-I core and ESCRT-II GLUE domain structures reveal role for GLUE in linking to ESCRT-I and membranes, Cell 125 (2006) 99–111.

[14] H. Teo, O. Perisic, B. Gonzalez, R.L. Williams, ESCRT-II, an endosome-associated complex required for protein sorting: crystal structure and interactions with ESCRT-III and membranes, Dev. Cell 7 (2004) 559–569.

[15] M. Babst, D.J. Katzmann, E.J. Estepa-Sabal, T. Meerloo, S.D. Emr, Escrt-III: an endosome-associated heterooligomeric protein complex required for mvb sorting, Dev. Cell 3 (2002) 271–282.

[16] P.I. Hanson, R. Roth, Y. Lin, J.E. Heuser, Plasma membrane deformation by circular arrays of ESCRT-III protein filaments, J. Cell Biol. 180 (2008) 389–402.

[17] M. Babst, B. Wendland, E.J. Estepa, S.D. Emr, The Vps4p AAA ATPase regulates membrane association of a Vps protein complex required for normal endosome function, EMBO J. 17 (1998) 2982–2993.

[18] J. Martin-Serrano, A. Yarovoy, D. Perez-Caballero, P.D. Bieniasz, Divergent retroviral late-budding domains recruit vacuolar protein sorting factors by using alternative adaptor proteins, Proc. Natl. Acad. Sci. U S A 100 (2003) 12414–12419.

[19] B. Strack, A. Calistri, S. Craig, E. Popova, H.G. Gottlinger, AIP1/ALIX is a binding partner for HIV-1 p6 and EIAV p9 functioning in virus budding, Cell 114 (2003) 689–699.

[20] U.K. von Schwedler, M. Stuchell, B. Muller, D.M. Ward, H.Y. Chung, E. Morita, H.E. Wang, T. Davis, G.P. He, D.M. Cimbora, A. Scott, H.G. Krausslich, J. Kaplan, S.G. Morham, W.I. Sundquist, The protein network of HIV budding, Cell 114 (2003) 701–713.

[21] D.G. Demirov, E.O. Freed, Retrovirus budding, Virus Res. 106 (2004) 87–102.

[22] J.E. Garrus, U.K. von Schwedler, O.W. Pornillos, S.G. Morham, K.H. Zavitz, H.E. Wang, D.A. Wettstein, K.M. Stray, M. Cote, R.L. Rich, D.G. Myszka, W.I. Sundquist, Tsg101 and the vacuolar protein sorting pathway are essential for HIV-1 budding, Cell 107 (2001) 55–65.

[23] R.D. Fisher, H.Y. Chung, Q. Zhai, H. Robinson, W.I. Sundquist, C.P. Hill, Structural and biochemical studies of ALIX/AIP1 and its role in retrovirus budding, Cell 128 (2007) 841–852.

[24] T. Watanabe, E.M. Sorensen, A. Naito, M. Schott, S. Kim, P. Ahlquist, Involvement of host cellular multivesicular body functions in hepatitis B virus budding, Proc. Natl. Acad. Sci. U S A 104 (2007) 10205−10210.
[25] M.C. Bonaldo, R.C. Garratt, P.S. Caufour, M.S. Freire, M.M. Rodrigues, R.S. Nussenzweig, R. Galler, Surface expression of an immunodominant malaria protein B cell epitope by yellow fever virus, J. Mol. Biol. 315 (2002) 873−885.
[26] C.M. Rice, A. Grakoui, R. Galler, T.J. Chambers, Transcription of infectious yellow fever RNA from full-length cDNA templates produced by in vitro ligation, New Biol. 1 (1989) 285−296.
[27] E. Hochuli, Large-scale chromatography of recombinant proteins, J. Chromatogr. 444 (1988) 293−302.
[28] M.W. Pfaffl, A new mathematical model for relative quantification in real-time RT-PCR, Nucleic Acids Res. 29 (2001) e45.
[29] O. Vincent, L. Rainbow, J. Tilburn, H.N. Arst Jr., M.A. Penalva, YPXL/I is a protein interaction motif recognized by *Aspergillus* PalA and its human homologue, AIP1/Alix, Mol. Cell Biol. 23 (2003) 1647−1655.
[30] C. Chen, O. Vincent, J. Jin, O.A. Weisz, R.C. Montelaro, Functions of early (AP-2) and late (AIP1/ALIX) endocytic proteins in equine infectious anemia virus budding, J. Biol. Chem. 280 (2005) 40474−40480.
[31] J. McCullough, R.D. Fisher, F.G. Whitby, W.I. Sundquist, C.P. Hill, ALIX-CHMP4 interactions in the human ESCRT pathway, Proc. Natl. Acad. Sci. U S A 105 (2008) 7687−7691.
[32] K. Katoh, H. Shibata, H. Suzuki, A. Nara, K. Ishidoh, E. Kominami, T. Yoshimori, M. Maki, The ALG-2-interacting protein Alix associates with CHMP4b, a human homologue of yeast Snf7 that is involved in multivesicular body sorting, J. Biol. Chem. 278 (2003) 39104−39113.
[33] J. Wu, A.K. Bera, R.J. Kuhn, J.L. Smith, Structure of the Flavivirus helicase: implications for catalytic activity, protein interactions, and proteolytic processing, J. Virol. 79 (2005) 10268−10277.
[34] J.L. Kim, K.A. Morgenstern, J.P. Griffith, M.D. Dwyer, J.A. Thomson, M.A. Murcko, C. Lin, P.R. Caron, Hepatitis C virus NS3 RNA helicase domain with a bound oligonucleotide: the crystal structure provides insights into the mode of unwinding, Structure 6 (1998) 89−100.
[35] C.T. Chiou, C.C. Hu, P.H. Chen, C.L. Liao, Y.L. Lin, J.J. Wang, Association of Japanese encephalitis virus NS3 protein with microtubules and tumour susceptibility gene 101 (TSG101) protein, J. Gen. Virol. 84 (2003) 2795−2805.
[36] V. Dussupt, M.P. Javid, G. Abou-Jaoude, J.A. Jadwin, J. de La Cruz, K. Nagashima, F. Bouamr, The nucleocapsid region of HIV-1 Gag cooperates with the PTAP and LYPXnL late domains to recruit the cellular machinery necessary for viral budding, PLoS Pathog. 5 (2009) e1000339.
[37] C. Wirblich, B. Bhattacharya, P. Roy, Nonstructural protein 3 of bluetongue virus assists virus release by recruiting ESCRT-I protein Tsg101, J. Virol. 80 (2006) 460−473.
[38] S.M. Amberg, C.M. Rice, Mutagenesis of the NS2B-NS3-mediated cleavage site in the flavivirus capsid protein demonstrates a requirement for coordinated processing, J. Virol. 73 (1999) 8083−8094.
[39] C.E. Stocks, M. Lobigs, Signal peptidase cleavage at the flavivirus C-prM junction: dependence on the viral NS2B-3 protease for efficient processing requires determinants in C, the signal peptide, and prM, J. Virol. 72 (1998) 2141−2149.
[40] T. Wollert, C. Wunder, J. Lippincott-Schwartz, J.H. Hurley, Membrane scission by the ESCRT-III complex, Nature 458 (2009) 172−177.
[41] C. Chatellard-Causse, B. Blot, N. Cristina, S. Torch, M. Missotten, R. Sadoul, Alix (ALG-2-interacting protein X), a protein involved in apoptosis, binds to endophilins and induces cytoplasmic vacuolization, J. Biol. Chem. 277 (2002) 29108−29115.
[42] J.L. Gallop, C.C. Jao, H.M. Kent, P.J. Butler, P.R. Evans, R. Langen, H.T. McMahon, Mechanism of endophilin N-BAR domain-mediated membrane curvature, EMBO J. 25 (2006) 2898−2910.
[43] M. Masuda, S. Takeda, M. Sone, T. Ohki, H. Mori, Y. Kamioka, N. Mochizuki, Endophilin BAR domain drives membrane curvature by two newly identified structure-based mechanisms, EMBO J. 25 (2006) 2889−2897.
[44] C. Notredame, D.G. Higgins, J. Heringa, T-Coffee: a novel method for fast and accurate multiple sequence alignment, J. Mol. Biol. 302 (2000) 205−217.